Aerodynamic Design Optimization of UAV Rotor Blades using a Genetic Algorithm

Hak-Min Lee[1], Nahm-Keon Hur[2] and *Oh-Joon Kwon[3]

[1], [3] *Department of Aerospace Engineering, KAIST, Daejeon 305-600, Korea*
[2] *Department of Mechanical Engineering, Sogang University, Seoul 121-742, Korea*
[1] *hmlee928@kaist.ac.kr*
[2] *nhur@sogang.ac.kr*
[3] *ojkwon@kaist.ac.kr*

ABSTRACT

In the present study, an aerodynamic design optimization of UAV rotor blades was conducted using a genetic algorithm (GA) coupled with computational fluid dynamics (CFD). To reduce computational cost in finding optimum value using a genetic algorithm, a function approximation was applied using artificial neural networks (ANN) based on a radial basis function. Three dimensional and compressible Reynolds-Averaged Navier-Stokes (RANS) flow solver was used to analyze the flow around UAV rotor blades. Design variables such as pitch angle, chord length and thickness were adopted to perform aerodynamic design optimization. The objective functions were specified to maximize thrust coefficient maintaining torque coefficient and minimize torque coefficient maintaining thrust coefficient In case of optimization minimizing torque coefficient, torque coefficient was decreased 5.5% comparing with baseline configuration. As a result of optimization regarding to maximizing thrust coefficient, thrust coefficient was increased 2.8% than that of baseline configuration.

1. INTRODUCTION

An unmanned aerial vehicle (UAV) is an aircraft with no human pilot aboard. UAVs were developed for military in the initial stage but nowadays used in a number of civil applications such as policing, filming and shipping. The power sources of UAVs are obtained from a tilt rotor or multi-rotors, turboprop engine. Among them, Multi-rotor UAVs are able to take off and land vertically like helicopter and it is easy to operate at the narrow space. Depending on increasing uses in many ways, the researches for multi-rotor UAV were conducted (Hoffmann, 2007, Bristeau, 2009, Hrishikeshavan, 2012). Also, the optimal design researches were performed to improve the performances of a rotor at the design stage. In the past, a few researches were performed to enhance performances of a rotor. Pape et al (2005) conducted the

---

[1] Graduate Student
[2], [3] Professor

optimization of helicopter rotor aerodynamic performance on hover. Fuglsang et al (1999) studied the optimization method for wind turbine.

In the present study, the optimization was performed based on the CFD technique to improve the performances of a rotor using a GA (Michalewicz, 1996) and ANN (McCulloch, 1943, Broomhed, 1988). Design variables such as pitch angle, chord length, and thickness were adopted to perform the design optimization. Two cases of design optimization were carried out. The objective functions were set to minimize torque coefficient maintain thrust coefficient and maximize thrust coefficient maintaining torque coefficient.

2. DESIGN OPTIMIZATION METHODS

Aerodynamic design optimization was conducted using a GA and ANN. In Fig 1, a detail flow chart of the optimization framework is shown. At first, the performances for the various geometries corresponding to the different design variables are predicted using the flow solver and collected to construct the initial database for the design variables and the object functions. The function based on the initial database is approximated by using learning procedure of ANN. Next, a GA is used to search the optimum point for the approximated function. Finally, optimum shape for the approximated function is validated by using the flow solver. When the difference limitation of between the performances of the ANN prediction and the flow solver is satisfied, the optimization procedure is completed. Otherwise, the CFD calculation result is added to the database, and optimization procedure is repeated until the ANN prediction is agreed to the CFD validation.
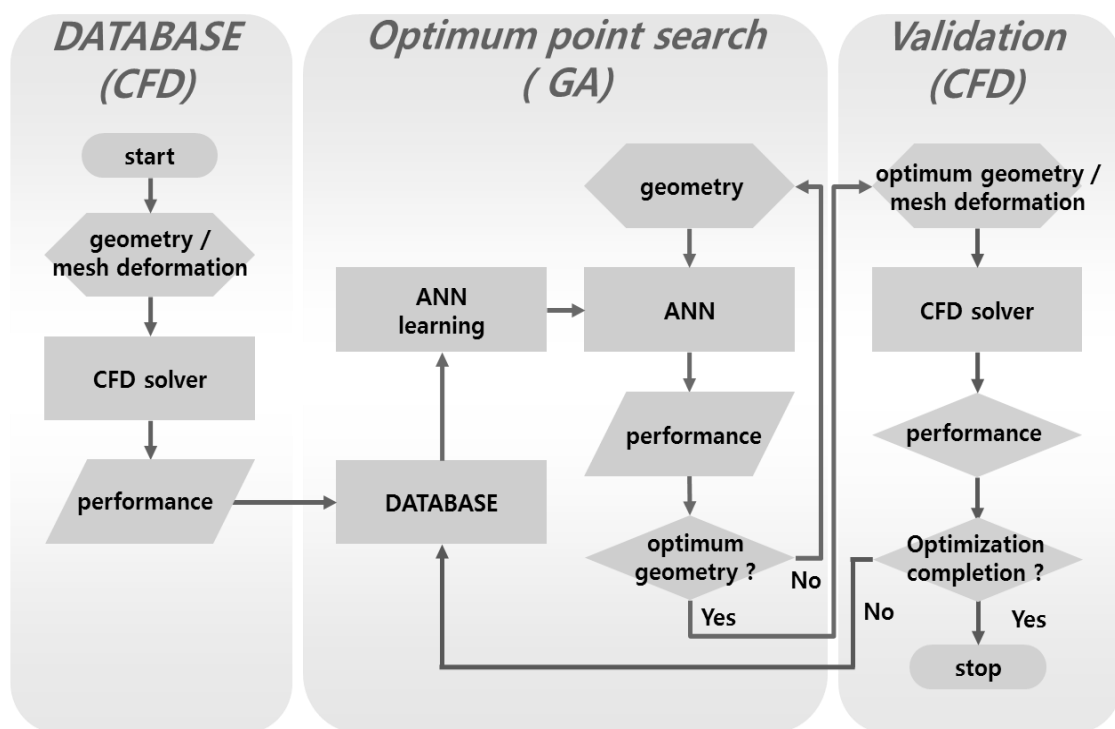

Fig. 1 Flowchart of design optimization

3. NUMERICAL METHOD

To analyze flow around multi-rotor UAV rotor blades, Reynolds-Averaged Navier-Stokes(RANS) equations which governs three-dimensional, viscous, compressible flows was used The governing equations may be written in an integral form for a bounded domain V with a boundary ∂V as

$$\frac{\partial}{\partial t}\int_V Q dV + \oint_{\partial V} \vec{F}(Q) \cdot \vec{n}\, dS = \int_{\partial V} \vec{G}(Q) \cdot \vec{n}\, dS + \int_V S(Q) dV \tag{1}$$

where $Q = [\rho, \rho u, \rho v, \rho w, e_0]^T$ is the vector of the conservative flow variables. The governing equations were discretized by using a vertex-centered finite-volume method on unstructured meshes. The inviscid flux, $F(Q)$, was calculated using Roe's flux difference splitting scheme (Roe, 1981), while the viscous flux, $G(Q)$, was computed by adopting a central differencing. The source term, $S(Q)$, was used for rotor blades rotating on a Z axis with constant rotating speed to reduce computational time. The flow solver was also coupled with a genetic algorithm to perform aerodynamic design optimization. The Spalart-Allmaras (1992) one-equation model was adopted for a turbulence modeling. The Venkatakrishnan (1995) limiter is used to prevent the non-physical oscillations. The flow solver was parallelized for the efficient calculation.
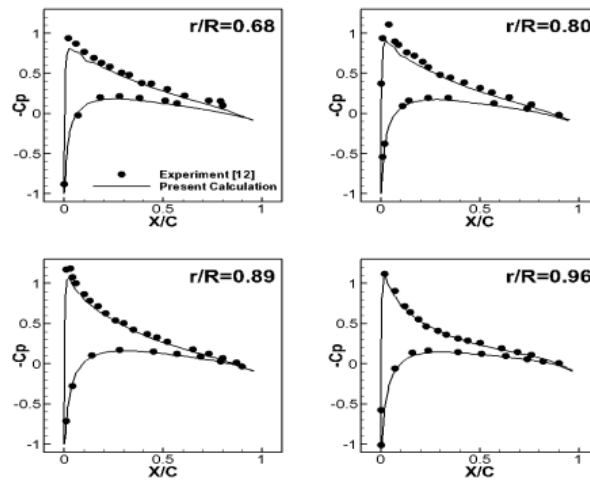

Fig. 2 Comparison of pressure coefficient distributions on Caradonna Tung rotor blade

4. RESULTS

4.1 VALIDATION OF FLOW SOLVER

For validation of flow solver, the calculations were made for Caradonna Tung rotor blade (Tung, 1984). The Reynolds number is 1,920,000 and tip Mach number of a rotor is 0.439. The results are compared with experimental data in Fig. 2. A good agreement is observed.

4.2 COMPUTATIONAL MESH

The geometry of a rotor is that the radius is 0.2m and the aspect ratio is 6.92. The computational mesh was generated as shown Fig. 3. A single blade was modelled using a periodic boundary condition. Prismatic cells of 18 layers were constructed. The grid spacing of the first layer was selected such that y^+ value was about unity. The remainder of the computational domain was constructed by using tetrahedral elements. The mesh consisted of 4.3 million cells and 1.4 million nodes.

(a) Surface   (b) Far field

Fig 3 Computational Mesh

4.3 DESIGN CONDITIONS

The flow conditions are shown in Table 1. The RPM range for Multi-rotor UAV is 5000 to 7000 RPM. Flow analysis was conducted at 6000 RPM. The design variables such as chord length, thickness, and pitch angle on five radial positions of 0.25R, 0.44R, 0.62R, 0.80R and 0.98R were used. To construct the initial database, the design variables were randomly selected using improved Latin hypercube method and the initial mesh was deformed within the range of design variables in Table 2. The number of the initial database is 800.

Table 1 Flow Condition

r/R	Pitch angle	Thickness	Chord length
0.80	1.09917	0.80001	1.19997
0.98	0.96035	0.80005	1.19988

Table 2 Range of design variables

Design variables	Minimum	Maximum
Pitch angle	-15%	10%
Thickness	-20%	10%
Chord length	-10%	20%

4.4 OPTIMIZATION RESULT

4.4.1 MINIMIZATION OF TORQUE

At first, the design optimization was conducted to minimize the torque. The performance before and after design optimization are summarized in Table 3. It is shown that significant improvement is obtained in the object function satisfying the constraints conditions such that thrust coefficient is similar to and the torque coefficient is smaller than those of the baseline Multi-rotor shape.

Table 3 Comparison of performances for optimization to minimize torque coefficient

	Initial shape	Optimized shape	Improvement rate
Thrust coefficient	0.010590	0.010520	0.7%
Torque coefficient	0.001125	0.001063	-5.5%
Figure of merit	0.685	0.718	4.8%

The sectional shapes of baseline and optimized rotors are presented in Fig 4 and the design variables of the optimized shape are summarized in Table 4. At the positions from 0.62r/R to 0.80r/R, the pitch angles of the optimized Multi-rotor shape are increased. On the other hand, the thicknesses are decreased to the lower limits of design variables at the positions from 0.44r/R to 0.98r/R. In case of the chord lengths, those are increased at all positions.
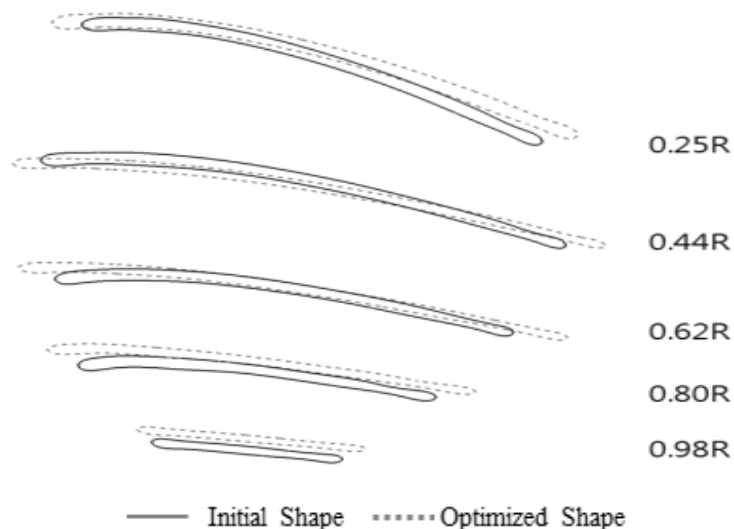

Fig 4 Comparison of reference sections before and after design optimization for minimization of thrust coefficient

Table 4 Design variables of optimized shape for minimization of thrust coefficient

r/R	Pitch angle	Thickness	Chord length
0.25	0.85010	1.09604	1.19029
0.44	0.85005	0.80026	1.11873
0.62	1.07461	0.80004	1.19899
0.80	1.09917	0.80001	1.19997
0.98	0.96035	0.80005	1.19988

For more detail analysis, the static pressure coefficients along the chord are presented at four stations of 0.273R, 0.5R, 0.7R and 0.9R in Fig 5. The pressure difference near mid chord at all reference sections and pitch angle at the 0.273R for optimized shape are smaller than those of baseline Multi-rotor configuration. Due to those features, the torque is decreased comparing to that of baseline configuration. To satisfy the constraint condition, the pressure difference near leading edge at the 0.5R and 0.7R and chord lengths at all reference sections for optimized shape are increased.
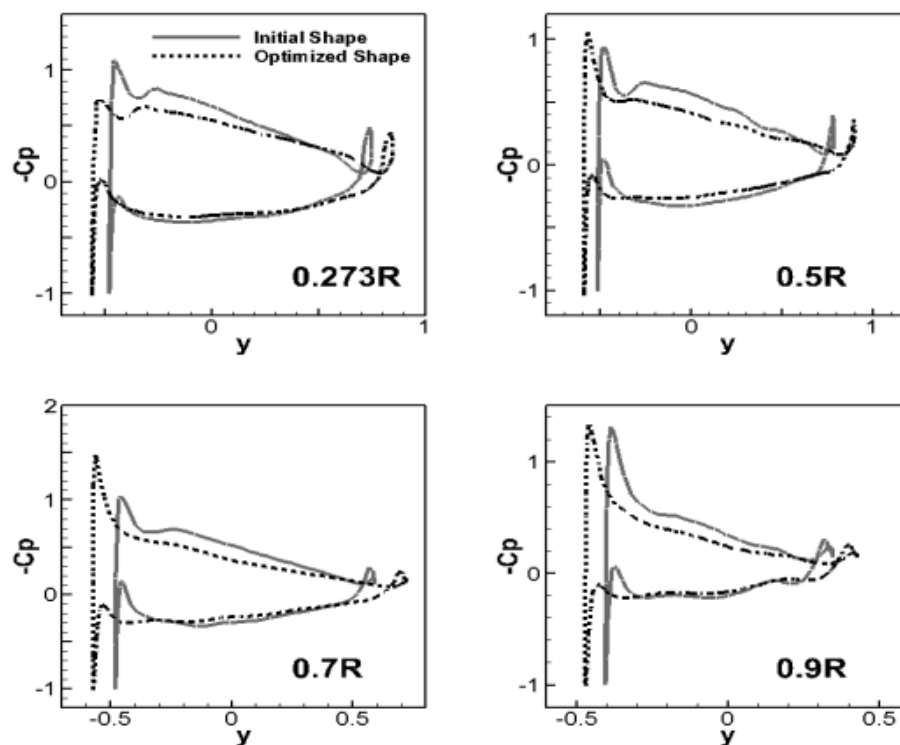

Fig 5 Comparison of pressure coefficient distributions before and after design optimization for minimization of thrust coefficient

4.4.2 MAXIMIZATION OF THRUST

Finally, the design optimization was conducted to maximize the thrust. The results of design optimization are summarized in Table 5. It is shown that the trust coefficient of the optimized Multi-rotor configuration is improved about 2.8% satisfying the constraints conditions such that the torque coefficient is similar to that of baseline configuration.

Table 5 Comparison of performances for optimization to minimize torque coefficient

	Initial shape	Optimized shape	Improvement rate
Thrust coefficient	0.010590	0.010890	2.8%
Torque coefficient	0.001125	0.001128	0.3%
Figure of merit	0.685	0.712	3.9%

In Fig 6, the sectional shapes of baseline and optimized rotor are presented. The design variables of the optimized shape are summarized in Table 6. For the optimized configuration, at the positions from 0.62r/R to 0.98r/R, the pitch angles are increased comparing to that of baseline configuration. And also the thickness is increased at 0.25r/R positions. In case of the chord lengths, as with the previous results of minimization of torque, those are increased at all positions.
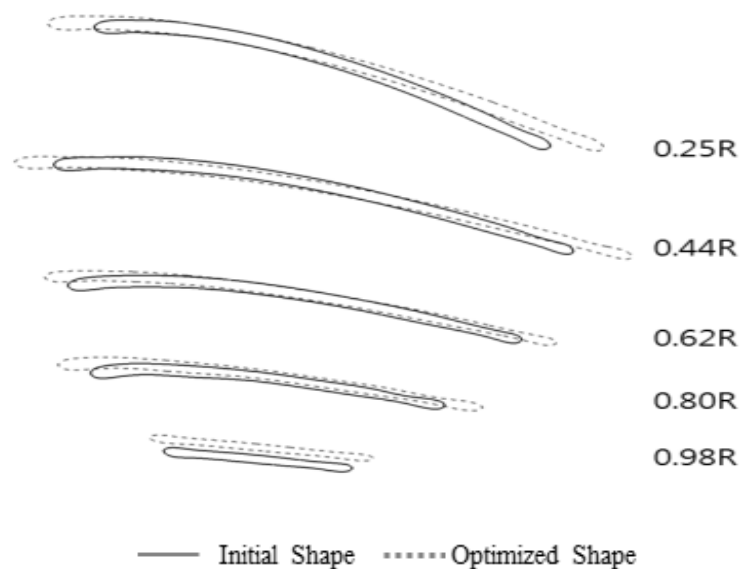

Fig 6 Comparison of reference sections before and after design optimization for maximization of thrust coefficient

Table 6 Design variables of optimized shape for maximization of thrust coefficient

r/R	Pitch angle	Thickness	Chord length
0.25	0.86421	1.02229	1.19844
0.44	0.90660	0.92405	1.18546
0.62	1.06320	0.83808	1.13060
0.80	1.09991	0.93932	1.19906
0.98	1.00341	0.80075	1.18638

The static pressure coefficients are compared in Fig. 7. The pressure difference near the leading edge at the 0.7R and chord length at all reference sections for optimized shape are larger than those of baseline configuration. Due to those features, the thrust is increased comparing to that of baseline configuration. To maintain the constraint, the pitch angle is reduced at the 0.273R and the pressure difference near mid chord for optimized shape is smaller than that of baseline configuration. As a results, the torque are maintained comparing to that of baseline shape.
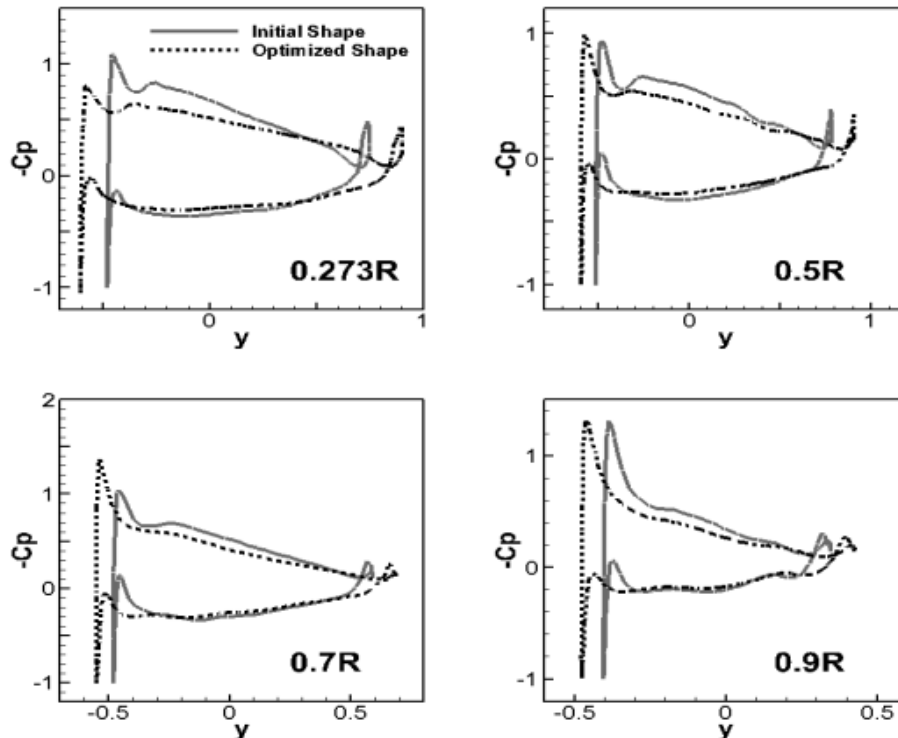

Fig 7 Comparison of pressure coefficient distributions before and after design optimization for maximization of thrust coefficient

5. CONCLUSION

In the present study, the optimization was conducted to enhance the performances of a rotor using a GA and ANN. To validate the flow solver, the calculations were performed for Caradonna Tung rotor. Design variables such pitch angle, chord length, and thickness were adopted to conduct the design optimization. The objective functions were specified to maximize thrust coefficient maintaining torque coefficient and minimize torque coefficient maintaining thrust coefficient In case of an optimization minimizing torque coefficient, torque coefficient was decreased 5.5% comparing with baseline configuration. As a result of an optimization regarding to maximizing thrust coefficient, thrust coefficient was increased 2.8% than that of baseline configuration.

ACKNOWLEDGMENTS

REFERENCES

Ale Pape and P.Beaumier. (2005), "Numerical optimization of helicopter rotor aerodynamic performance on hover" Aerospace Science and Technology 9(2005) 191-201

Broomhed, D.S., and Lowe, D. (1988), "Radial basis function, multi-variable functional interpolation and adaptive networks", Technical Report RSME Memorandum, Royal Signals and Radar Establishment, 1988, (4148).

Bristeau, P-J., Martin, P., Salaun, E., and Petit, N. (2009) , "The Role of Propeller Aerodynamics in the Model of a Quadrotor UAV," Proceedings of the European Control Conference, Budapest, Hungary, 2009, pp. 683–688.

Hoffmann, G. M., Huang, H. and Waslander, S. L. (2007), and Tomlin, C. J., "Quadrotor Helicopter Flight Dynamics and Control: Theory and Experiment," AIAA Guidance, Navigation, and Control Conference, AIAA Paper 2007-6461, Aug. 2007.

Hrishikeshavan, V., Black, J., and Chopra, I. (2012), "Design and Testing of a Quad Shrouded Rotor Micro Air Vehicle in Hover," 53rd AIAA Structural Dynamics and Materials Conference, AIAA Paper 2012-1720, April 2012.

McCulloch, W.S., and Pitts, W. (1943), "A logical calculus of ideas immanent in nervous activity", Bulletin of Mathematical Biophysics, 1943, 5, pp.115-133.

Michalewicz, Z. (1996), "Genetic algorithms + data structures = evolution programs", (Springer, 1996).

P. Fuglsang and HA Madsen. (1999), "Optimization method for wind turbine rotors" Journal of Wind Engineering and industrial Aerodynamics volume 80. Issues 1-2. 1 March 1999, pages 191-206

Roe, P.L. (1981), "Approximate Riemann Solvers, Parameter Vectors and Difference

Scheme", Journal of Computational Physics, Vol.43, 1981, pp.357-372.

Spalart, P.R., and Allmaras, S.R. (1902), "A One-Equation turbulent Model for Aerodynamic Flows", AIAA 92-0439, 1992.

Tung, C., Caradonna, F., and Johnson, W. (1984). "The Prediction of Transonic Flows on an Advancing Rotor," American Helicopter Society 40th Annual Forum, Arlington, VA, USA.

Venkatakrishnan, V. (1995), "Convergence to Steady State Solutions of the Euler Equations on Unstructured Grids with Limiters", Journal of Computational Physics, Vol.118, No.1, 1995, pp.120-130.